

Resolving an apparent discrepancy between theory and experiment: spin–spin coupling constants for FCCF

Janet E. Del Bene,^{a*} Patricio F. Provasi,^b Ibon Alkorta^c and José Elguero^c

Ab initio equation of motion coupled cluster singles and doubles (EOM–CCSD) and second-order polarization propagator approximation (SOPPA) calculations have been performed to evaluate spin–spin coupling constants for FCCF (difluoroethyne). The computed EOM–CCSD value of $^3J(\text{F–F})$ obtained at the experimental geometry of this molecule supports the previously reported experimental value of 2.1 Hz, thereby resolving an apparent discrepancy between theory and experiment. This coupling constant exhibits a strong dependence on the C–C and C–F distances, and its small positive value results from a sensitive balance of paramagnetic spin-orbit (PSO) and spin-dipole (SD) terms. The three other unique FCCF coupling constants $^1J(\text{C–C})$, $^1J(\text{C–F})$, and $^2J(\text{C–F})$ have also been reported and compared with experimental data. While $^1J(\text{C–F})$ is in agreement with experiment, the computed value of $^2J(\text{C–F})$ is larger than our estimate of the experimental coupling constant. Copyright © 2008 John Wiley & Sons, Ltd.

Keywords: difluoroethyne; spin–spin coupling constants; EOM–CCSD; SOPPA

Introduction

Previous theoretical studies of spin–spin coupling constants for FCCF (difluoroethyne) have reported significantly different values of $^3J(\text{F–F})$. These range from -85.4 Hz from semiempirical calculations,^[1] -43.7 ^[2] and -21.5 Hz^[3] from second-order polarization propagator approximation (SOPPA) calculations, and -25.4 Hz from an earlier equation of motion coupled cluster singles and doubles (EOM–CCSD) calculation.^[4] The computed results prompted the authors of Ref. [2] to question the assignment of the experimental spectrum of FCCF, which yielded a value of 2.1 Hz for $^3J(\text{F–F})$,^[5] although the sign of this coupling constant was not determined. In an effort to resolve this discrepancy, we have reinvestigated spin–spin coupling in FCCF, with emphasis on $^3J(\text{F–F})$. We have recently reported a systematic study of spin–spin coupling constants in a series of singly bonded molecules $\text{H}_m\text{X–YH}_n$, with $\text{X, Y} = \text{C, N, O, F}$, and selected fluoro-derivatives.^[6] In that study, we noted that computed EOM–CCSD coupling constants are in better agreement with experimental values than SOPPA coupling constants, and that the SOPPA values could be significantly in error for couplings involving O and F. In the course of that study, we also noted that there can be a significant geometry dependence of some computed coupling constants. In the present study, we investigate both the method and geometry dependence of spin–spin coupling constants for FCCF.

Methods

Coupling constants were computed for FCCF using the EOM–CCSD method in the configuration interaction (CI)-like approximation^[7–10] with all electrons correlated, and the SOPPA method,^[11–15] employing the Ahlrichs qzp basis set^[16] on ^{13}C and ^{19}F . Both EOM–CCSD and SOPPA explicitly include electron

correlation effects, which have increased importance for coupling involving the more electronegative atoms, with EOM–CCSD providing a higher level of treatment. These calculations were initially carried out on the optimized geometries of FCCF obtained at second-order Møller–Plesset perturbation theory (MP2)^[17–20] with the 6-31+G(d,p),^[21–24] 6-311++G(d,p),^[25] and aug-cc-pVTZ^[26,27] basis sets, and at the coupled cluster singles and doubles with noniterative inclusion of triples [CCSD(T)]^[28,29] geometry using the aug-cc-pVTZ basis set. In addition, to minimize the effect of the neglect of zero-point motion for such structures, we have performed these same calculations at the experimental FCCF geometry.^[30] All terms which contribute to the total coupling constant, namely, the paramagnetic spin-orbit (PSO), diamagnetic spin-orbit (DSO), Fermi-contact (FC), and spin-dipole (SD), have been evaluated.

We have also investigated in detail the distance dependence of $^3J(\text{F–F})$ and its components at EOM–CCSD, and have computed a two-dimensional EOM–CCSD grid of $^3J(\text{F–F})$ values by changing the experimental C–C distance of 1.1865 Å by ± 0.04 Å in steps of 0.02 Å, and the two C–F distances of 1.2832 Å by ± 0.02 Å in steps of 0.01 Å. These increments were chosen so that each step along the C–C and C–F axes changes the F–F distance by the same amount, 0.02 Å. Structure optimizations were done with Gaussian 03.^[31] The EOM–CCSD calculations were done with ACES II^[32] on the Itanium Cluster at the Ohio Supercomputer Center, while the

* Correspondence to: Janet E. Del Bene, Department of Chemistry, Youngstown State University, Youngstown, Ohio 44555, USA. E-mail: jedelbene@ysu.edu

^a Department of Chemistry, Youngstown State University, Youngstown, Ohio 44555, USA

^b Department of Physics, University of Northeastern, Av. Libertad 5500, W 3404 AAS Corrientes, Argentina

^c Instituto de Química Médica, CSIC, Juan de la Cierva, 3, E-28006 Madrid, Spain

Table 1. Optimized and experimental C–C and C–F distances (Å) for FCCF

Method ^a	R(C–C)	R(C–F)	R(F–F)
MP2/6-31+G(d,p)	1.2026	1.3050	3.8126
MP2/6-311++G(d,p)	1.1973	1.2867	3.7707
MP2/aug-cc-pVTZ	1.1946	1.2870	3.7686
CCSD(T)/aug-cc-pVTZ	1.1928	1.2895	3.7718
Experimental ^b	1.1865	1.2832	3.7529

^a The basis sets are listed in order of increasing size.
^b Ref. [30].

SOPPA calculations were performed using Dalton 2^[33] on IQM computers.

Results and Discussion

Table 1 presents the optimized MP2/6-31+G(d,p), MP2/6-311++G(d,p), MP2/aug-cc-pVTZ, and CCSD(T)/aug-cc-pVTZ geometries and the experimental geometry of FCCF. From Table 1 it can be seen that the computed C–C and C–F distances at all levels of theory overestimate the experimental distances, with the largest discrepancies found at MP2/6-31+G(d,p). Since the computed distances are too long, applying zero-point vibrational corrections would not improve agreement with experiment. Table 2 presents values of $^1J(\text{C–C})$, $^1J(\text{C–F})$, $^2J(\text{C–F})$, and $^3J(\text{F–F})$ computed at these geometries, as well as the experimental coupling constants.

$^3J(\text{F–F})$

From Table 2 it can be seen that $^3J(\text{F–F})$ is large and negative at the computed geometries, but as the C–C and C–F distances (and therefore the F–F distance) decrease and approach the experimental distances, $^3J(\text{F–F})$ increases (becomes less negative). The SOPPA values at the computed geometries are -42.7 , -18.4 , -17.5 , and -19.6 Hz at MP2/6-31+G(d,p), MP2/6-311++G(d,p), MP2/aug-cc-pVTZ, and CCSD(T)/aug-cc-pVTZ, respectively. The EOM–CCSD coupling constants are consistently smaller in absolute value at -25.3 , -5.3 , -4.8 , and -6.8 Hz, respectively. At the experimental geometry of FCCF, the computed SOPPA value of $^3J(\text{F–F})$ is -9.5 Hz, while the EOM–CCSD coupling constant changes sign and is equal to $+1.4$ Hz. This value is in good agreement with the experimental value of 2.1 Hz. Thus, the EOM–CCSD calculation at the experimental geometry of FCCF supports the original experimental assignment of this coupling constant given in Ref. [5]. Moreover, we have also reevaluated this coupling constant from the experimental spectrum and obtained a value of 2.2 Hz. The sign of this coupling constant has not been determined. Although the agreement between the SOPPA value of $^3J(\text{F–F})$ and the experimental value is improved when the experimental geometry is used for the calculation, it is not as good as the agreement between the EOM–CCSD and the experimental coupling constant. As noted previously,^[6] describing couplings involving F requires the use of a method that provides an improved description of electron correlation effects if agreement with experiment is to be achieved.

It is apparent from Table 2 that $^3J(\text{F–F})$ is sensitive to changes in C–C and C–F distances, so we have investigated this sensitivity in detail at EOM–CCSD. Figure 1 illustrates the dependence of

Table 2. Spin–spin coupling constants (Hz) for FCCF at various geometries^a

Geometry	$^1J(\text{C–C})$		$^1J(\text{C–F})$	
	SOPPA	EOM–CCSD	SOPPA	EOM–CCSD
MP2/6-31+G(d,p)	436.3	422.9	-357.1	-311.2
MP2/6-311++G(d,p)	432.1	418.8	-331.9	-289.2
MP2/aug-cc-pVTZ	431.9	418.8	-329.8	-287.5
CCSD(T)/aug-cc-pVTZ	432.2	419.2	-331.2	-288.9
Experimental geometry ^b	430.2	417.5	-318.3	-277.7
Experimental J	–	–	–	-287.3^c

Geometry	$^2J(\text{C–F})$		$^3J(\text{F–F})$	
	SOPPA	EOM–CCSD	SOPPA	EOM–CCSD
MP2/6-31+G(d,p)	31.3	33.1	-42.7	-25.3
MP2/6-311++G(d,p)	38.0	39.9	-18.4	-5.3
MP2/aug-cc-pVTZ	37.5	39.5	-17.5	-4.8
CCSD(T)/aug-cc-pVTZ	36.2	38.3	-19.6	-6.8
Experimental geometry ^b	37.9	40.2	-9.5	1.4
Experimental J	–	28.7^d	–	2.1^c

^a The listing is in order of increasing size of the basis set.
^b Experimental geometry from Ref. [30].
^c Ref. [5].
^d Our value.

$^3J(\text{F–F})$ and its PSO, FC, and SD components on the C–C distance, with the C–F distances fixed at the experimental value. The DSO term is nearly constant and has a value of approximately -2 Hz. The sign and magnitude of $^3J(\text{F–F})$ are determined as a result of a competition between a large and positive SD term which remains nearly constant with distance, and a negative PSO term which decreases (has a larger negative value) as the C–C distance increases. At short distances the SD term dominates, while at longer distances the PSO term is the dominant one. The FC term is relatively small and positive, and remains nearly constant with distance. The dependence of $^3J(\text{F–F})$ on the C–F distances with the C–C distance fixed at its experimental value is illustrated in Fig. 2. As the C–F distances increase, the F–F distance increases, and the negative PSO term decreases faster than the positive SD term. Thus, $^3J(\text{F–F})$ is positive at shorter distances and negative at longer distances. The experimental value of 2.1 Hz for $^3J(\text{F–F})$ results from a sensitive balance of PSO and SD terms.

Shown in Fig. 3 is the $^3J(\text{F–F})$ coupling surface constructed on a 25-point grid. This surface was constructed assuming a linear dependence on each distance and including a cross-term. The color coding presents a pictorial description of the curvature of this surface. At the center of the grid is the value of 1.4 Hz computed at the experimental geometry. Going from left to right across a grid line increases each C–F distance by 0.04 Å, thereby increasing the F–F distance by 0.08 Å. As the C–F distance increases $^3J(\text{F–F})$ decreases by 35.0 , 37.0 , 39.2 , 41.4 , and 43.8 Hz at C–C distances of 1.1465 , 1.1665 , 1.1865 , 1.2065 , and 1.2265 Å, respectively. Along this coordinate, the F–F distance increases from 3.7129 to 3.7929 Å in steps of 0.02 Å. At all C–C distances, $^3J(\text{F–F})$ changes sign as the C–F distance increases. Going from the back to the front of the grid at a given C–F distance increases the C–C and F–F distances by 0.08 Å, and $^3J(\text{F–F})$ decreases by 19.1 , 21.3 , 23.5 , 25.7 , and

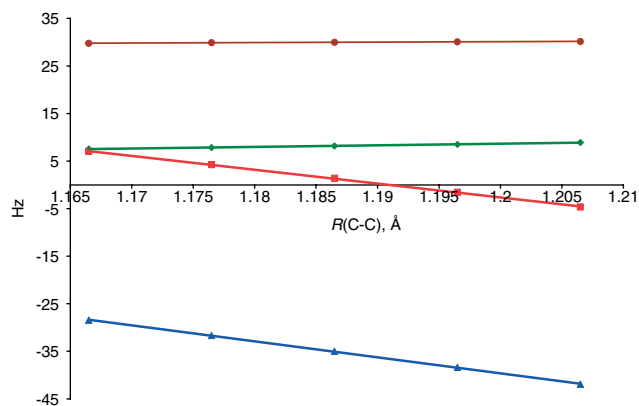


Figure 1. EOM-CCSD values of the PSO (\blacktriangle), FC (\blacklozenge), and SD (\bullet) terms and $^3J(F-F)$ (\blacksquare) versus the C-C distance at the experimental C-F distance.

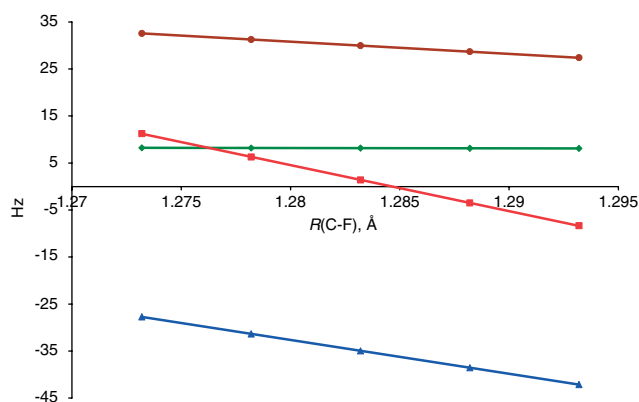


Figure 2. EOM-CCSD values of the PSO (\blacktriangle), FC (\blacklozenge), and SD (\bullet) terms and $^3J(F-F)$ (\blacksquare) versus the C-F distance at the experimental C-C distance.

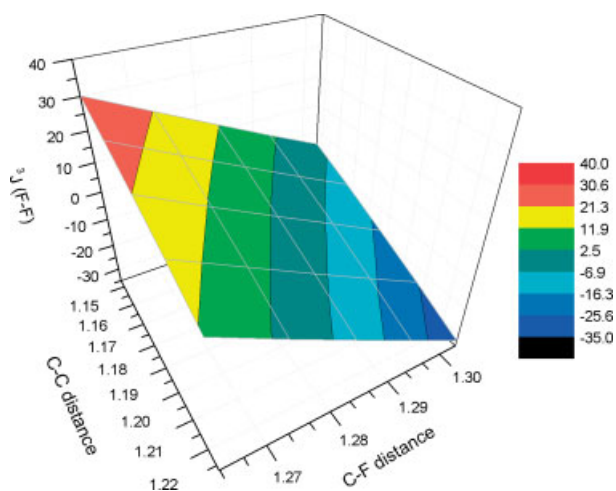


Figure 3. $^3J(F-F)$ coupling surface as a function of C-C and C-F distances.

27.9 Hz at C-F distances of 1.2632, 1.2732, 1.2832, 1.2932, and 1.3032 Å, respectively, and again the F-F distance increases from 3.7129 to 3.7929 Å. At the shortest C-F distance, $^3J(F-F)$ decreases with increasing C-C distance but does not change sign. However, as the C-F distances increase, a change of sign is observed for $^3J(F-F)$.

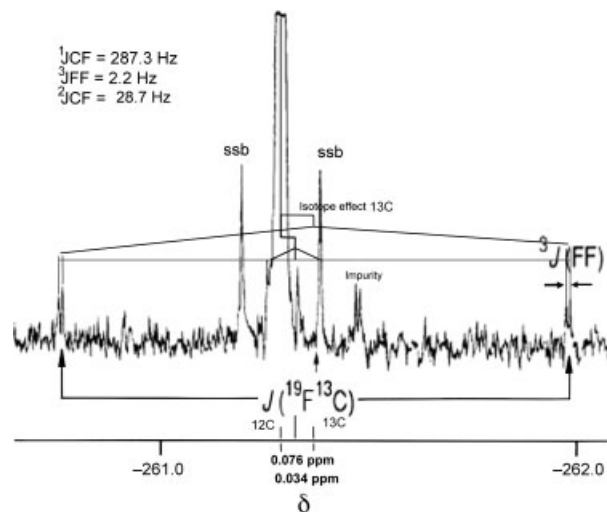


Figure 4. The ^{19}F NMR spectrum of FCCF from Ref. [5], with notations added.

The largest change in the F-F distance (0.16 Å) occurs along the diagonal going from the bottom left of the grid to the top right as both the C-C and C-F distances increase. Not surprisingly, the largest decrease in $^3J(F-F)$ of 62.9 Hz is found along this diagonal. In contrast, going along the diagonal from top left to bottom right increases the C-F distances but decreases the C-C distance while keeping the F-F distance constant. Nevertheless, $^3J(F-F)$ decreases by 15.9 Hz, indicating that this coupling constant is more sensitive to the C-F than C-C distance.

$^1J(C-C)$, $^1J(C-F)$, and $^2J(C-F)$

There are three other unique coupling constants for FCCF, $^1J(C-C)$, $^1J(C-F)$, and $^2J(C-F)$, and these are reported in Table 2. $^1J(C-C)$ changes only slightly with geometry, varying from 436.3 to 430.2 Hz at SOPPA, and from 422.9 to 417.5 Hz at EOM-CCSD. The computed SOPPA values are always greater than the EOM-CCSD values. There is no experimental value available for this coupling constant.

$^1J(C-F)$ shows a much greater dependence on geometry. At SOPPA, it varies from -357.1 Hz at MP2/6-31+G(d,p) to -318.3 Hz at the experimental geometry. At EOM-CCSD, $^1J(C-F)$ varies from -311.2 to -277.7 Hz. The value at the experimental geometry is in agreement with the experimental coupling constant of -287.3 Hz.^[4]

Not surprisingly, $^2J(C-F)$ is also sensitive to the C-C and C-F distances, but it tends to increase as these distances decrease. It varies from 31.3 to 38.0 Hz at SOPPA, and from 33.1 to 40.2 Hz at EOM-CCSD. Since no experimental value for $^2J(C-F)$ has been reported, we have estimated this coupling constant from Fig. 4 and obtained a value of +28.7 Hz. Thus, at the experimental geometry, the computed SOPPA and EOM-CCSD values overestimate the experimental coupling constant by approximately 10 Hz.

Conclusions

The computed EOM-CCSD F-F coupling constant $^3J(F-F)$ for FCCF obtained at the experimental geometry of this molecule supports the experimental value of 2.1 Hz, thereby resolving what appeared to be a discrepancy between theory and experiment.

This coupling constant exhibits a strong dependence on the C–C and C–F distances, and also on the level of treatment of electron correlation effects. The small positive value of ${}^3J(\text{F–F})$ at EOM–CCSD results from a sensitive balance of a negative PSO and a positive SD term, with the former dominating at longer distances, and the latter at shorter distances. Three other unique FCCF coupling constants ${}^1J(\text{C–C})$, ${}^1J(\text{C–F})$, and ${}^2J(\text{C–F})$ are reported, and an estimate of ${}^2J(\text{C–F})$ has been made on the basis of its experimental NMR spectrum. The EOM–CCSD value of ${}^1J(\text{C–F})$ is in agreement with experiment, but the computed value of ${}^2J(\text{C–F})$ overestimates the estimated experimental value. Why this is the case is a subject for future study. No experimental data are available for ${}^1J(\text{C–C})$. For comparison purposes, results of corresponding SOPPA calculations on FCCF are also included.

Experimental Measurements

Bürger *et al.* reported the following data for FCCF^[5]: ${}^1J(^{19}\text{F–}^{13}\text{C}) = 287.3$ Hz; ${}^3J(^{19}\text{F–}^{19}\text{F}) = 2.1$ Hz (sign not determined); isotope effect $\Delta\delta^{19}\text{F}(^{12}\text{C}) = \delta^{19}\text{F}(^{12}\text{C}) - \delta^{19}\text{F}(^{13}\text{C}) = 0.08$ ppm. Bürger and Eugen (personal communication, May 2008) confirmed these values after adjusting the isotope effect to 0.076 ppm. From the spectrum reported in Ref. [5], we have measured ${}^3J(^{19}\text{F–}^{19}\text{F}) = 2.2$ Hz. Assuming that the isotope effect on the other fluorine atom is much lower than 0.076 ppm, we have estimated a value of ${}^2J(\text{C–F})$ of 28.7 Hz, as indicated in Fig. 4. Using these values of the three coupling constants (irrespective of their sign), we have produced a simulated spectrum, which matches the experimental spectrum.

Acknowledgements

The authors acknowledge the continuing support of the Ohio Supercomputer Center (JEDB); and financial support from CONICET, FONCYT (PICT 21604/2004 and PAE 22592/2004), and UNNE (PFP); and from the Spanish Ministerio de Educación y Ciencia (Project No. CTQ2007-61901/BQU) and Comunidad Autónoma de Madrid (Project MADRISOLAR, ref S-0505/PPQ/0225) (JE and IA).

References

- [1] K. Hirao, H. Nakatsuji, H. Kato, T. Yonezawa, *J. Am. Chem. Soc.* **1972**, *94*, 4078.
- [2] P. F. Provasi, G. A. Aucar, S. P. A. Sauer, *J. Phys. Chem. A* **2004**, *108*, 5393.
- [3] P. F. Sanchez, G. A. Provasi, G. A. Aucar, S. P. A. Sauer, *Adv. Quantum Chem.* **2005**, *48*, 161.
- [4] J. E. Del Bene, I. Alkorta, J. Elguero, *Z. Phys. Chem.* **2003**, *217*, 1565.
- [5] H. Bürger, S. Sommer, *J. Chem. Soc., Chem. Commun.* **1991**, *7*, 456.
- [6] J. E. Del Bene, I. Alkorta, J. Elguero, *J. Chem. Theory Comput.* **2008**, *4*, 967.
- [7] S. A. Perera, H. Sekino, R. J. Bartlett, *J. Chem. Phys.* **1994**, *101*, 2186.
- [8] S. A. Perera, M. Nooijen, R. J. Bartlett, *J. Chem. Phys.* **1996**, *104*, 3290.
- [9] S. A. Perera, R. J. Bartlett, *J. Am. Chem. Soc.* **1995**, *117*, 8476.
- [10] S. A. Perera, R. J. Bartlett, *J. Am. Chem. Soc.* **1996**, *118*, 7849.
- [11] T. Enevoldsen, J. Oddershede, S. P. A. Sauer, *Theor. Chem. Acc.* **1998**, *100*, 275.

- [12] (a) J. Geertsen, J. Oddershede, G. E. Scuseria, *J. Chem. Phys.* **1987**, *87*, 2138; (b) J. Oddershede, J. Geertsen, G. E. Scuseria, *J. Phys. Chem.* **1988**, *92*, 3056.
- [13] (a) E. S. Nielsen, P. Jørgensen, J. Oddershede, *J. Chem. Phys.* **1980**, *73*, 6238; (b) J. Oddershede, P. Jørgensen, D. L. Yeager, *Comput. Phys. Rep.* **1984**, *2*, 33.
- [14] M. J. Packer, E. K. Dalskov, T. Enevoldsen, H. J. Aa. Jensen, J. Oddershede, *J. Chem. Phys.* **1996**, *105*, 5886.
- [15] E. K. Dalskov, S. P. A. Sauer, *J. Phys. Chem. A* **1998**, *102*, 5269.
- [16] A. Schäfer, H. Horn, R. Ahlrichs, *J. Chem. Phys.* **1992**, *97*, 2571.
- [17] J. A. Pople, J. S. Binkley, R. Seeger, *Int. J. Quantum Chem. Quantum Chem. Symp.* **1976**, *10*, 1.
- [18] R. Krishnan, J. A. Pople, *Int. J. Quantum Chem.* **1978**, *14*, 91.
- [19] R. J. Bartlett, D. M. Silver, *J. Chem. Phys.* **1975**, *62*, 3258.
- [20] R. J. Bartlett, G. D. Purvis, *Int. J. Quantum Chem.* **1978**, *14*, 561.
- [21] W. J. Hehre, R. Ditchfield, J. A. Pople, *J. Chem. Phys.* **1982**, *56*, 2257.
- [22] P. C. Hariharan, J. A. Pople, *Theor. Chim. Acta* **1973**, *238*, 213.
- [23] G. W. Spitznagel, T. Clark, J. Chandrasekhar, P. v. R. Schleyer, *J. Comput. Chem.* **1982**, *3*, 3633.
- [24] T. Clark, J. Chandrasekhar, G. W. Spitznagel, P. v. R. Schleyer, *J. Comput. Chem.* **1983**, *4*, 294.
- [25] R. Krishnan, J. S. Binkley, R. Seeger, J. A. Pople, *J. Chem. Phys.* **1980**, *72*, 650.
- [26] T. H. Dunning Jr, *J. Chem. Phys.* **1989**, *90*, 1007.
- [27] D. E. Woon, T. H. Dunning Jr, *J. Chem. Phys.* **1995**, *103*, 4572.
- [28] K. Raghavachari, G. W. Trucks, J. A. Pople, M. Head-Gordon, *Chem. Phys. Lett.* **1989**, *157*, 479.
- [29] R. J. Bartlett, J. D. Watts, S. A. Kucharski, J. Noga, *Chem. Phys. Lett.* **1990**, *165*, 513.
- [30] H. Bürger, W. Schneider, S. Sommer, W. Thiel, *J. Chem. Phys.* **1991**, *95*, 660.
- [31] M. J. Frisch, G. W. Trucks, H. B. Schlegel, G. E. Scuseria, M. A. Robb, J. R. Cheeseman, J. A. Montgomery Jr, T. Vreven, K. N. Kudin, J. C. Burant, J. M. Millam, S. S. Iyengar, J. Tomasi, V. Barone, B. Mennucci, M. Cossi, G. Scalmani, N. Rega, G. A. Petersson, H. Nakatsuji, M. Hada, M. Ehara, K. Toyota, R. Fukuda, J. Hasegawa, M. Ishida, T. Nakajima, Y. Honda, O. Kitao, H. Nakai, M. Klene, X. Li, J. E. Knox, H. P. Hratchian, J. B. Cross, C. Adao, J. Jaramill, R. Gomperts, R. E. Stratmann, O. Yazyev, A. J. Austin, R. Cammi, C. Pomelli, J. W. Ochterski, P. Y. Ayala, K. Morokuma, G. A. Voth, P. Salvador, J. J. Dannenberg, V. G. Zakrzewski, S. Dapprich, A. D. Daniels, M. C. Strain, O. Farkas, D. K. Malick, A. D. Rabuck, K. Raghavachari, J. B. Foresman, J. V. Ortiz, Q. Cui, A. G. Baboul, S. Clifford, J. Cioslowski, B. B. Stefanov, G. Liu, A. Liashenko, P. Piskorz, I. Komaromi, R. L. Martin, D. J. Fox, T. Keith, M. A. Al-Laham, C. Y. Peng, A. Nanayakkara, M. Challacombe, P. M. W. Gill, B. Johnson, W. Chen, M. W. Wong, C. Gonzalez, J. A. Pople, *Gaussian 03, Revision C.02*, Gaussian, Inc.: Wallingford, **2004**.
- [32] J. F. Stanton, J. Gauss, J. D. Watts, M. Nooijen, N. Oliphant, S. A. Perera, P. G. Szalay, W. J. Lauderdale, S. R. Gwaltney, S. Beck, A. Balkova, D. E. Bernholdt, K. K. Baeck, P. Tozyczko, H. Setkino, C. Huber, R. J. Bartlett, Integral packages included are VMOL (J. Almlöf, P. R. Taylor), VPROPS (P. R. Taylor), ABACUS (T. Helgaker, H. J. Aa. Jensen, P. Jørgensen, J. Olsen, P. R. Taylor), Brillouin–Wigner perturbation theory was implemented by J. Pittner, *ACES II is a Program Product of the Quantum Theory Project*, University of Florida.
- [33] C. Angeli, K. L. Bak, V. Bakken, O. Christiansen, R. Cimraglia, S. Coriana, P. Dahle, E. K. Dalskov, T. Enevoldsen, B. Fernandez, C. Hättig, K. Hald, A. Halkier, H. Heiberg, T. Helgaker, H. Hettema, H. J. Aa. Jensen, D. Honsson, P. Jørgensen, S. Kirpekar, W. Klopper, R. Kobayashi, H. Koch, A. Ligabue, O. B. Lutnæs, K. V. Mikkelsen, P. Norman, J. Olsen, M. J. Packer, T. B. Pedersen, Z. Rinkevicius, E. Rudberg, T. A. Ruden, K. Ruud, P. Salek, A. Sanchez de Meras, T. Saue, S. P. A. Sauer, B. Schimmelpfennig, K. O. Sylvester-Hvid, P. R. Taylor, O. Vahtras, D. J. Wilson, H. Ågren, DALTON, a molecular electronic structural program, Release 2.0, <http://www.kjemi.uio.no/software/dalton/dalton.htm>, **2005**.